Climate Dynamics (1993) 9:53–61

Climate Dynamics

On the cold start problem in transient simulations with coupled atmosphere-ocean models

Klaus Hasselmann[1], **Robert Sausen**[2], **Ernst Maier-Reimer**[1], **Reinhard Voss**[3]

[1] Max-Planck-Institut für Meteorologie, Bundesstrasse 55, D-20146 Hamburg, Germany
[2] Deutsche Forschungsanstalt für Luft- und Raumfahrt, Institut für Physik der Atmosphäre, Postfach 1116, D-82230 Wessling, Germany
[3] Meteorologisches Institut der Universität Hamburg, Bundesstrasse 55, D-20146 Hamburg, Germany

Received: April 1992/Accepted: 8 February 1993

Abstract. Finite computer resources force compromises in the design of transient numerical experiments with coupled atmosphere-ocean general circulation models which, in the case of global warming simulations, normally preclude a full integration from the undisturbed pre-industrial state. The start of the integration at a later time from a climate state which, in contrast to the true climate, is initially in equilibrium then induces a cold start error. Using linear response theory a general expression for the cold start error is derived. The theory is applied to the Hamburg CO_2 scenario simulations. An attempt to estimate the global-mean-temperature response function of the coupled model from the response of the model to a CO_2 doubling was unsuccessful because of the non-linearity of the system. However, an alternative derivation, based on the transient simulation itself, yielded a cold start error which explained the initial retardation of the Hamburg global warming curve relative to the IPCC results obtained with a simple box-diffusion-upwelling model. In the case of the sea level the behaviour of the model is apparently more linear. The cold start error estimations based on a CO_2 doubling experiment and on an experiment with gradually increasing CO_2 (scenario A) are very similar and explain about two thirds of the coupled model retardation relative to the IPCC results.

1 Introduction

It has long been recognized that the global warming due to the continual build-up of greenhouse gas concentrations in the atmosphere cannot be computed reliably as the quasi-instantaneous equilibrium climate response with the aid of atmospheric general circulation models (A-GCMs) alone, but must be treated as a transient problem using coupled atmosphere-ocean general circulation models (A-O-GCMs). It is only recently, however, that global ocean models have become sufficiently realistic and super-computers sufficiently powerful to carry out such simulations with acceptable resolution over longer time periods. Computer resources, nevertheless, still represent a serious limitation in such computations. None of the greenhouse scenario simulations which have been recently completed (Washington and Meehl 1989; Stouffer et al. 1989; Cubasch et al. 1992) has been able to span the full period of the build-up of greenhouse gases, beginning in the early nineteenth century, while also extending the integration over a similar time period into the future. To limit computer time, the initial state in such global warming simulations is normally taken as an equilibrium state at some time close to the present.

The difference between such a "cold start" simulation and a preferable, but too costly, "warm-up" simulation beginning in the early nineteenth century is indicated schematically in Fig. 1. We assume that in both

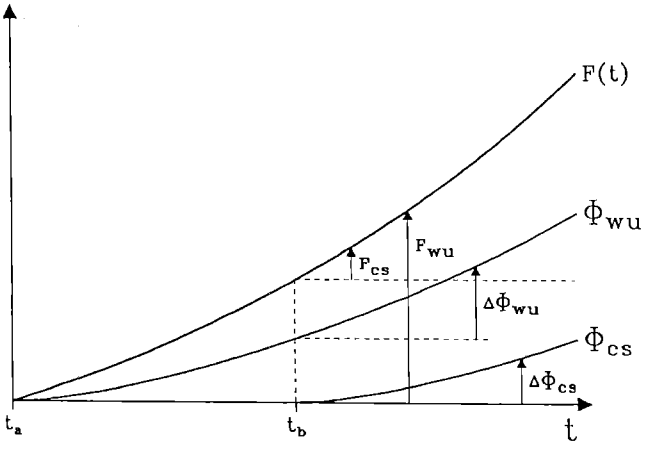

Fig. 1. Definition of the cold start-problem. Φ_{wu} and Φ_{cs} denote the responses to the forcings F_{wu} and F_{cs}, respectively. The change since time t_b is larger for the warm-up case "*wu*" than for the cold start case "*cs*"

Correspondence to: R Sausen

simulations the quantity of interest is the change in the climate state $\vec{\Phi}(t)$ relative to the climate state at some recent reference time $t=t_b$ (for example 1985). In the warm-up simulation, the changing climate evolves from an equilibrium initial state at time $t=t_a$ at the beginning of the greenhouse gas buildup (e.g. 1820), while in the cold start simulation the global warming and greenhouse gas build-up are considered relative to an assumed equilibrium initial state at time t_b. We wish to determine the difference between the computed change in climate $\Delta\vec{\Phi}(t)=\vec{\Phi}(t)-\vec{\Phi}(t_b)$ in the period $t>t_b$ for the cold start and warm-up simulations.

The cold start simulation will generally underestimate the climate change, since in this simulation the initial rate of change of the climate state at time $t=t_b$ is zero, while in the warm-up simulation a finite derivative has already developed at $t=t_b$. A comparison of the global warming predictions from coupled atmosphere-ocean simulations beginning in 1985 (Cubasch et al. 1992) with the corresponding estimates from simple box-diffusion-upwelling models beginning in the last century (e.g. Houghton et al. 1990) does indeed indicate an underestimate of several tenths of a degree (or a factor of the order of 2) of the coupled model simulations during the first few decades. Similar underpredictions relative to the box-diffusion-upwelling model are found in other O-A-GCM simulations (e.g. Washington and Meehl 1989; Murphy 1991, personal communication). The predictions generally lie closer to the box-model results at later times, when the start-up errors are small compared with the total warming. The question then arises whether the differences between the computed initial responses of the coupled atmosphere-ocean and simple box-diffusion-upwelling models reflect real differences in the models or are simply a consequence of the different initial conditions. Since the predicted global warming in the next few decades is of particular concern for policy makers, quantification of the cold start errors in recently published atmosphere-ocean model simulations is of considerable interest.

It will be shown in this study that the errors can be rigorously determined within the approximation of linear response theory. The impulse response function can be inferred from an independent step function response experiment. Most modelling groups carry out such experiments as a tool for studying the transient response charcteristics of the coupled atmosphere-ocean system, so that the corrections can be readily made. The impulse response function can also be inferred from the greenhouse warming experiment itself, although this is less straightforward than the analysis of a step function response experiment. However, it turns out, that in our application to the Cubasch et al. (1992) global warming experiments, the second method is more appropriate. A CO_2 doubling experiment available as step function response was of too large amplitude to be regarded as a small perturbation of the initial state. The non-linear model response to a CO_2 doubling is found to be significantly different from the response to a slow increase of the CO_2 concentration.

The general cold start error expression is derived in the following section and is then computed for a number of examples in Section 3. The global mean temperature correction for the Hamburg IPCC scenarios A and D simulations (Cubasch et al. 1992) is found to be in the order of 0.2 K if the CO_2 doubling experiment is used to determine the impulse response function. However, it is of the order 0.5 K if the transient warming simulation itself is used to determine the response function characteristics. The latter estimate, which is regarded as the more appropriate, explains most of the retardation found in the Hamburg experiments relative to the IPCC predictions. Nevertheless, another mechanism, e.g. a stronger initial heat uptake by the ocean, or a transient natural interdecadal fluctuation of the coupled atmosphere-ocean system, as discussed by Cubasch et al. (1992), could also have contributed to the retardation.

Since completion of this study we have received an independent analysis of the cold start problem by Wigley and Raper (personal communication 1991), who use a similar approach, but applied to a special single-time-constant feedback climate model. This model happens to be included as an example in Section 3.1. It yields a cold start correction comparable to the correction computed from the response function inferred empirically from the coupled atmosphere-ocean model response to a gradual CO_2 increase.

2 The cold start error

In the following we consider perturbations of a climate system about an equilibrium reference state which are sufficiently small to be linearized. The linear approximation can be assumed to apply at least during the initial period of a global warming simulation, with which we shall be primarily concerned in the estimation of the cold start error.

Let $\vec{R}(t)$ denote the linear transient response of the climate model (for example an A-O-GCM) to a unit step function forcing at time $t=0$ (Fig. 2, top panel). Then the linear response of the climate state $\vec{\Phi}$ to an arbitrary forcing $F(t)$ (with $F(t)=0$ for $t\leq 0$) is given by

$$\vec{\Phi}(t)=\int_0^t \frac{dF}{du}(u)\,\vec{R}(t-u)\,du \tag{1}$$

$$=\int_0^t F(u)\,\vec{G}(t-u)\,du \tag{2}$$

where $\vec{G}(t)=\dfrac{d\vec{R}}{dt}$ is the impulse response (Green) function (Fig. 2, bottom panel).

It is assumed in (1), (2) that the input forcing function $F(t)$ is a scalar function, whereas the response $\vec{\Phi}(t)$ is taken as the complete climate state vector. Equations (1), (2) can be readily generalized to a vector input, in which case the response function $\vec{R}(t)$ and $\vec{G}(t)$ would represent matrices. In our applications $F(t)$ will represent the change in radiative forcing due

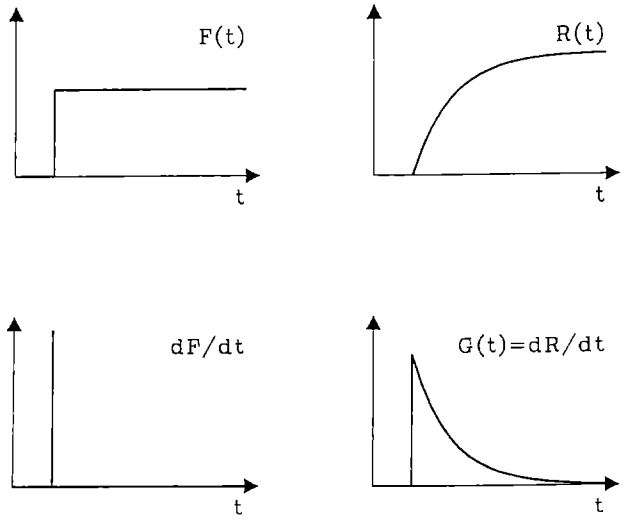

Fig. 2. *Upper panel:* step function forcing (*left*) and associated response (*right*); *Lower panel:* derivative of a step function forcing (*left*) and impulse response (Green) function (*right*)

to a change in the global mean greenhouse gas concentrations (expressed in terms of an equivalent CO_2 concentration), and as climate response variables we will consider, as examples, the global mean near surface (2 m) temperature $T(t)$ and the global mean sea level rise $h(t)$.

The cold start error is defined through the difference between two response experiments (Fig. 1):

1. a warm-up experiment (*wu*) with a climate response $\vec{\Phi}_{wu}(t)$, in which the forcing $F_{wu} \equiv F(t)$ is turned on at a time $t = t_a$ (corresponding to the beginning of the greenhouse gas increase in the early nineteenth century), and
2. a cold-start experiment (*cs*) with a climate response $\vec{\Phi}_{cs}(t)$, in which the forcing $F_{cs}(t)$ is turned on at the time $t = t_b > t_a$ and is set equal to the deviation from the forcing of the warm-up experiment at the time t_b, i.e.

$$F_{cs}(t) = F(t) - F(t_b). \tag{3}$$

We compare now in both experiments the climate change $\Delta\vec{\Phi}$ for the period $t > t_b$ relative to the climate state at the time t_b (see Fig. 1):

$$\begin{aligned}\Delta\vec{\Phi}_{wu}(t) &= \vec{\Phi}_{wu}(t) - \vec{\Phi}_{wu}(t_b) \\ &= \int_{t_a}^{t} F(u)\,\vec{G}(t-u)\,du - \int_{t_a}^{t_b} F(u)\,\vec{G}(t_b-u)\,du \\ &= \int_{t_a}^{t_b} F(u)\,[\vec{G}(t-u) - \vec{G}(t_b-u)]\,du \\ &\quad + \int_{t_b}^{t} F(u)\,\vec{G}(t-u)\,du,\end{aligned} \tag{4}$$

$$\begin{aligned}\Delta\vec{\Phi}_{cs}(t) &= \vec{\Phi}_{cs}(t) \\ &= \int_{t_b}^{t} [F(u) - F(t_b)]\,\vec{G}(t-u)\,du.\end{aligned} \tag{5}$$

The difference between the climate change predicted in the two experiments is accordingly

$$\begin{aligned}\delta\vec{\Phi}(t) &= \Delta\vec{\Phi}_{cs}(t) - \Delta\vec{\Phi}_{wu}(t) \\ &= -\int_{t_a}^{t_b} F(u)[\vec{G}(t-u) - \vec{G}(t_b-u)]\,du \\ &\quad - F(t_b)\,\vec{R}(t-t_b).\end{aligned} \tag{6}$$

For $t \to \infty$ the impulse response function $\vec{G}(t)$ approaches zero and the response function $\vec{R}(t)$ approaches a constant. Thus, the cold start error $\delta\vec{\Phi}(t)$ also asymptotically approaches a constant.

3 Examples

3.1 Box model response

Consider a single climate variable $\vec{\Phi} = \Phi$ evolving according to a simple feedback equation

$$\frac{d\Phi}{dt} = -\lambda\Phi + \alpha \cdot F \tag{7}$$

where α, λ are constants. The response function ($\vec{R} = R$, $\vec{G} = G$) for this system is given by

$$R(t) = \frac{\alpha}{\lambda}(1 - e^{-\lambda t}) \tag{8}$$

or

$$G(t) = \alpha e^{-\lambda t}. \tag{9}$$

This single-time-constant model corresponds to T.M.C. Wigley and S.C.B. Raper's (personal communication) recent analysis of the cold start problem.

Equation (6) yields in this case

$$\begin{aligned}\delta\Phi(t) &= -\alpha \int_{t_a}^{t_b} F(u)[e^{-\lambda(t-u)} - e^{-\lambda(t_b-u)}]\,du \\ &\quad - \frac{\alpha}{\lambda} F(t_b)(1 - e^{-\lambda(t-t_b)}) \\ &= \frac{\alpha}{\lambda}[1 - e^{-\lambda(t-t_b)}] \\ &\quad \times \left[\lambda e^{-\lambda t_b} \int_{t_a}^{t_b} F(u)\,e^{\lambda u}\,du - F(t_b)\right]\end{aligned} \tag{10}$$

or

$$\delta\Phi(t) = -R(t-t_b)\,K(t_b - t_a) \tag{11}$$

where

$$K(t_b - t_a) = -\lambda e^{-\lambda t_b} \int_{t_a}^{t_b} F(u)\,e^{\lambda u}\,du + F(t_b). \tag{12}$$

Assume further that $F(t)$ grows linearly in time,

$$F(t) = F_0\beta[t - t_a] \tag{13}$$

where F_0 is the total radiative forcing at the time $t = t_a$, and $F(t)$ is the change in the radiative forcing since the time t_a. In this case the factor K [Eq. (12)] is given by

$$K(t_b - t_a) = \frac{F_0\beta}{\lambda}[1 - e^{-\lambda(t_b - t_a)}]. \tag{14}$$

To illustrate this example with some typical numbers, let the equivalent CO_2 concentration c increase exponentially with a growth rate of 1.3% per year (approxi-

mately ICPP "business as usual" scenerio = scenario A), i.e.

$$c(t) = c_a e^{\gamma(t-t_a)} \tag{15}$$

where $\gamma = 0.013\ a^{-1}$ and c_a is the concentration at time t_a, so that the CO_2 radiative forcing, which is approximately proportional to the logarithm of the concentration, increases linearly,

$$F(t) = F_1 \gamma [t - t_a]. \tag{16}$$

Choossing $F_1 = 1/\ln 2$, it follows that $F(t) = 1$ for a CO_2 doubling, which occurs at $t - t_a = 53$ years. If the equilibrium response to CO_2 doubling is 3 K and the e-folding time with which the model relaxes to this equilibrium is 20 years, i.e. $\lambda = 0.05\ a^{-1}$, it follows from (8) that $\alpha/\lambda = 3$ K.

If we start from equilibrium at $t = t_b$, the transient response of our model to the forcing given by Eq. (16) is

$$\begin{aligned} \Delta T(t) &= \int_{t_b}^{t} e^{-\lambda(t-u)}\, \alpha [F(u) - F(t_b)]\, du \\ &= \alpha F_1 \gamma \int_{t_b}^{t} e^{-\lambda(t-u)} (u - t_b)\, du \\ &= \frac{F_1 \gamma \alpha}{\lambda} \left[t - t_b - \frac{1 - e^{-\lambda(t-t_b)}}{\lambda} \right], \end{aligned} \tag{17}$$

while

$$K(t_b - t_a) = \frac{F_1 \lambda}{\lambda} [1 - e^{-\lambda(t_b - t_a)}]. \tag{18}$$

Figure 3 shows the response $\Delta T(t)$ and the cold start error $\delta T(t, t_b - t_a)$ for several time lags $t_b - t_a$.

3.2 Representation of the response function in terms of normal modes

For any non-degenerate linear system the response can be represented as a linear superposition of the response of individul modes with complex eigenvalues, $\mu_j = \lambda_j - i\omega_j$,

$$G(t) = \sum_j \alpha_j e^{-\mu_j t} \equiv \sum_j G_j(t) \tag{19}$$

$$R(t) = \sum_j \frac{\alpha_j}{\mu_j} (1 - e^{-\mu_j t}) \equiv \sum_j R_j(t) \tag{20}$$

Real eigenvalues ($\omega_j = 0$) occur singly, whereas complex eigenvalues ($\omega_j \neq 0$) occur in complex conjugate pairs (j_1, j_2) with $\mu_{j_1} = (\mu_{j_2})^*$, $\alpha_{j_1} = (\alpha_{j_2})^*$.

Substituting the general response functions (19), (20) into Eqs. (11), (12), we obtain

$$\delta\vec{\Phi}(t) = -\sum_j R_j(t - t_b)\, K_j(t_b - t_a) \tag{21}$$

where

$$K_j(t_b - t_a) = -\mu_j e^{-\mu_j t_b} \int_{t_a}^{t_b} F(u)\, e^{\mu_j u}\, du + F(t_b). \tag{22}$$

Equations (19), (20) are useful for fitting a (smoothed) approximate analytical representation to the response of a coupled atmosphere-ocean model which has been determined empirically from numerical experiments.

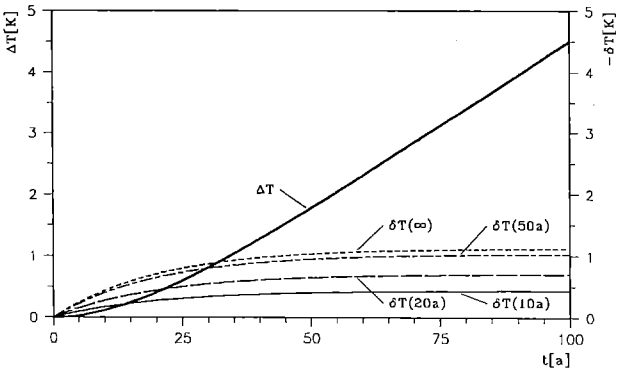

Fig. 3. Temperature response ΔT (*heavy line*) to linear forcing in the cold start case and the underestimation $-\delta T$ (*thin lines*) of the (true) warm-up response for several warm-up times ($t_b - t_a = 10$ a, 20 a, 50 a, ∞)

A similar representation of a numerically determined response function as a superposition of exponentials was used by Maier-Reimer and Hasselmann (1987) to describe the atmospheric CO_2 response to increasing CO_2 emissions computed with a three-dimensional carbon cycle model. The analytical representation was subsequently used by Wigley (1991), and by Wigley and Raper (personal communication) in conjunction with simple box-diffusion climate models to simulate the net climatic response to CO_2 emissions.

4 Application to coupled atmosphere-ocean model simulations

In the following we estimate the cold start errors incured in the simulations made by Cubasch et al. (1992) with the Hamburg coupled atmosphere-ocean model ECHAM-1/LSG for various CO_2 scenarios. In two of the simulations, it was assumed that the atmospheric equivalent CO_2 concentration increased according to the IPCC scenarios A and D (Houghton et al. 1990). In a third simulation, the response to an instantaneous increase of the equivalent CO_2 concentration from 390 ppm to 720 ppm was studied. Thus the $2 \times CO_2$ value of 720 ppm equivalent CO_2 concentration represents a doubling of the equivalent CO_2 concentration relative to the level of the early 1980s, rather than 1985. Finally, a control simulation was carried out with the equivalent CO_2 concentration fixed at 390 ppm. Each of the simulations started at time $t = t_b$ (1985) from an equilibrium (390 ppm) state of the coupled model (cold start). Figure 4 shows the equivalent CO_2 concentration used in the four simulations after 1985 (Houghton et al. 1990) and the evolution of the observed concentration from 1850 to 1985.

The global warming simulated by Cubasch et al. (1992) is plotted in Fig. 5 together with the "best estimate" IPCC box-diffusion-upwelling model predic-

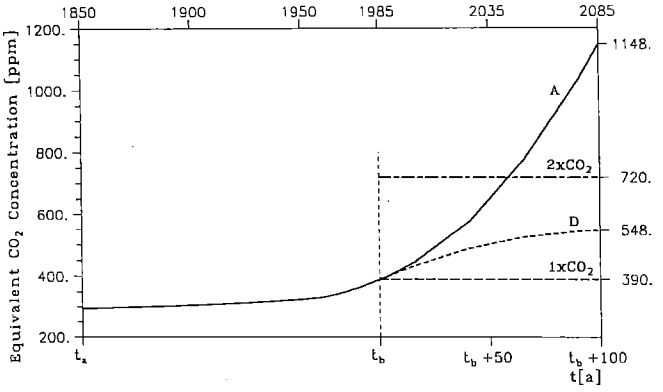

Fig. 4. Equivalent CO_2 concentrations for scenarios A and D, the instantaneous CO_2 "doubling", and the control simulation from Houghton et al. (1990)

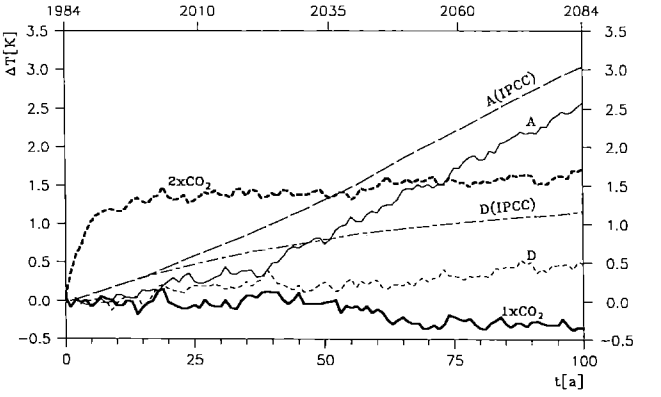

Fig. 5. Change of the global mean near surface (2 m) temperature due to increased CO_2 concentration as simulated with ECHAM-1/LSG (scenarios A and D, "$2\times CO_2$", and "$1\times CO_2$" = control) and as estimated by IPCC (scenarios A and D). All changes are defined relative to the mean of the years 1–10 of the control simulation

Table 1. Eigenvalues and amplitudes of the response function for the temperature derived from the "$2\times CO_2$" experiment, and the corresponding factors K_j for $t_b - t_a = 135$ a

j	μ_j [a^{-1}]	α_j/μ_j [K]	K_j
1	1/ 2.86	1.084	0.109
2	1/41.67	0.498	0.256

tions (Houghton et al. 1990) for scenarios A and D. The change in temperature is defined relative to the mean of the years 1–10 of the control simulation (definition 1 of Cubasch et al. 1992). The ECHAM-1/LSG response is seen to be considerably lower than the IPCC box-diffusion-upwelling model response for the first 40 years for both scenarios A and D.

To decide whether this initial depression is due to the cold start in 1985, we applied the analysis of Section 2. First, linear response functions were fitted to the "$2\times CO_2$" curve in Fig. 5. A good approximation is given by the sum

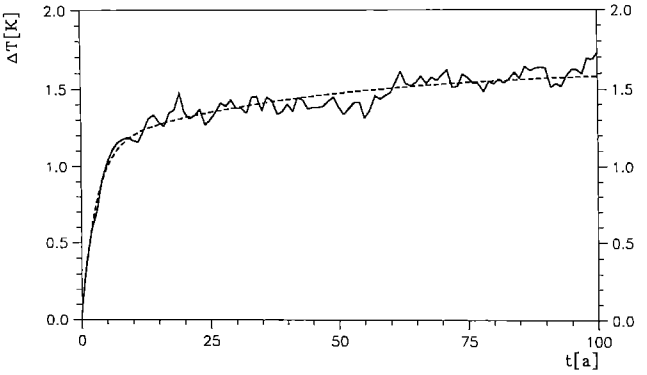

Fig. 6. Temperature response of the coupled model ECHAM-1/LSG to an instantaneous CO_2 "doubling" (*solid line*) and its approximation by a two-exponential linear response model (*dashed line*)

$$R_T(t) = \sum_{j=1}^{2} \frac{\alpha_j}{\mu_j}(1 - e^{-\mu_j t}) \tag{23}$$

of two exponentials with the parameters listed in the second and third columns of Table 1. The rms error of this approximation is 0.06 K (Fig. 6).

The CO_2 forcing is assumed to be proportional to the logarithm of the concentration:

$$F(t) = \frac{\ln(c(t)/c_a)}{\ln(c_2/c_b)} \tag{24}$$

where $c(t)$ is the CO_2 concentration at time t, c_a and c_b are the concentrations at times t_a and t_b, respectively and c_2 is the concentration of the "$2\times CO_2$" experiment. Denoting the forcing of the "$2\times CO_2$" experiment by

$$F_2 = \frac{\ln(c_2/c_a)}{\ln(c_2/c_b)} \tag{25}$$

the change in CO_2 forcing to the control simulation is

$$F_2 - F(t_b) = 1. \tag{26}$$

Taking $t_a = 1850$ and $t_b = 1985$, Eq. (22) yields the partial factors K_j listed in the last column of Table 1.

The temperature cold start error computed from (23) and (24) is plotted in Fig. 7. For large simulation times the temperature error δT approaches the asymptotic value of -0.25 K. The error is small relative to the simulated warming (see Fig. 5) and is unable to explain the retardation simulated by ECHAM-1/LSG.

For comparison, we investigated also the cold start error of the GFLD coupled A-O-GCM greenhouse warming simulations (Manabe et al. 1990). Their "$2\times CO_2$" curve (Fig. 9 of Manabe et al. 1990) can be approximated by

$$R_T(t) = \sum_{j=1}^{2} \frac{\alpha_j}{\mu_j}(1 - e^{-\mu_j t}) \tag{27}$$

with the parameters listed in Table 2. The rms error of the fit is 0.10 K. The resulting cold start error approaches -0.35 K for long simulation times.

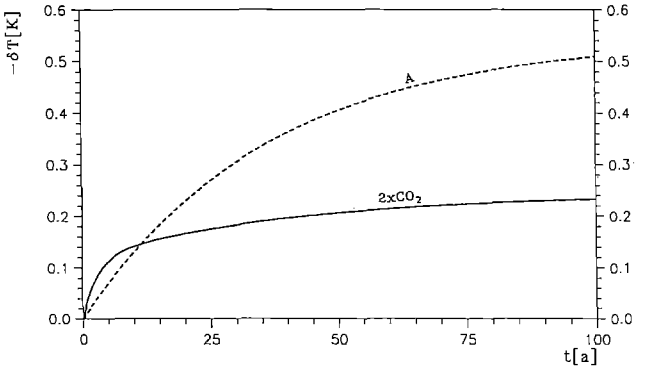

Fig. 7. Cold start temperature errors for the model ECHAM-1/LSG determined from the impulse response function inferred from the "$2\times CO_2$" experiment (*solid line*) and from the scenario A simulation (*dashed line*)

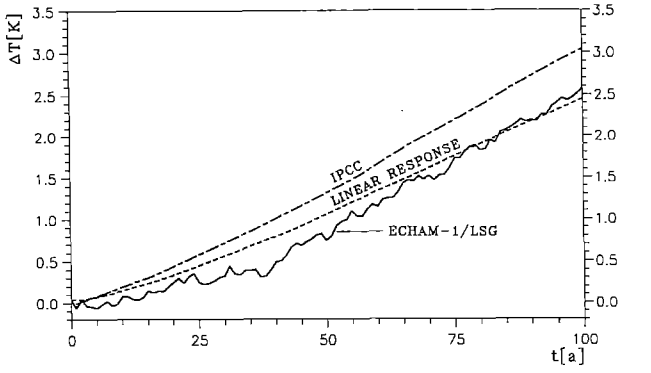

Fig. 8. Temperature response of the coupled model ECHAM-1/LSG for scenario A, its approximation by the linear response model inferred from the "$2\times CO_2$" experiment and the estimated IPCC response

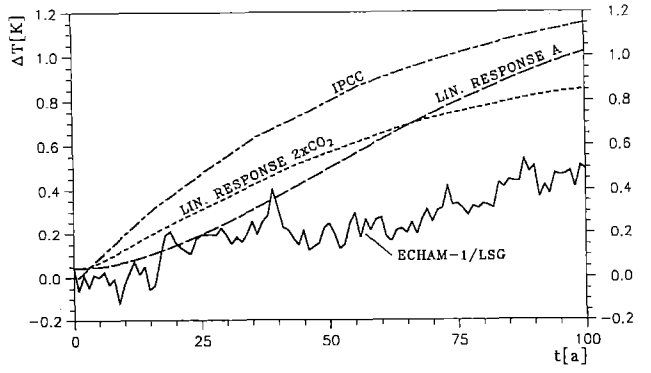

Fig. 9. Temperature response of the coupled model ECHAM-1/LSG for scenario D, its approximations by the linear response models inferred from the "$2\times CO_2$" experiment and the scenario A simulation, and the estimated IPCC response

As an independent test of the linear response function concept the response of the coupled atmosphere-ocean model to increasing CO_2 was computed for scenarios A and D directly from the input atmospheric CO_2 levels using the general linear response relation (2), with $G(t-u)$ given by the fitted form (19):

$$\Delta T_{lin}(t) = \sum_{j=1}^{2} \int_{t_b}^{t} F(u)\, G_j(t-u)\, du \qquad (28)$$

The resulting response (Figs. 8 and 9) does not reproduce the initial retardation of the temperature rise found in the full non-linear coupled atmosphere-ocean GCM simulation and in the case of scenario D significantly overestimates the response also for larger times. Thus the warming delay must either be attributed to the internal variability of the model, as discussed in Cubasch et al. (1992), or the equivalent linear response function derived from the "$2\times CO_2$" experiment yields an inappropriate description of the response to a gradual CO_2 increase – or both factors contribute to the deviations.

It appears probable that at least the second factor is important and that the deviation between the computed linear and the coupled atmosphere-ocean model response is mainly due to a non-linearity in the response of the sudden CO_2 doubling experiment from which the linear response properties were inferred. The amplitude of the "$2\times CO_2$" global temperature response is indeed larger than the response in the scenarios A and D during the initial period, for which the linear response relation was needed. Thus a non-linear distortion is more likely to arise in the "$2\times CO_2$" experiment than in the initial period of the scenarios A and D simulations. Physically, the non-linearity can be explained by the production of a stable warm mixed layer in the high latitude ocean when the warming in the "$2\times CO_2$" experiment is suddenly switched on, thereby inhibiting the subsequent penetration of heat into the deep ocean (see also Cubasch et al. 1992).

To circumvent this problem, an independent estimate of the cold start error was computed using an impulse response function inferred from the response to the scenerio A CO_2 increase. A good approximation to the linear response function (rms error is 0.06 K, see Fig. 10) was achieved with just one exponential, whose eigenvalue and amplitude are listed in Table 3. The resulting cold start error is plotted in Fig. 7. After 50 years the error is −0.41 K, which is substantially larger than the cold start error inferred from the impulse response function that was derived from the $2\times CO_2$ experiment. For a very long simulation time t the cold start error approaches the asymptotic value of −0.56 K.

After correction for this revised cold start error, most of the warming delay is seen to be removed

Table 2. Eigenvalues and amplitudes of the response function for the temperature derived from the GFDL "$2\times CO_2$" experiment, and the corresponding partial factors K_j

j	μ_j [a^{-1}]	α_j/μ_j [K]	K_j
1	1/ 1.2	0.872	0.177
2	1/23.5	0.973	0.198

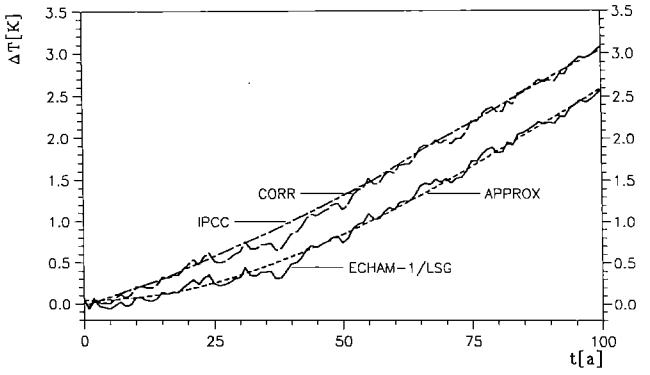

Fig. 10. Temperature response for scenario A: simulation by ECHAM-1/LSG, estimation by IPCC, approximation of the ECHAM-1/LSG curve by a fit (*APPROX*), and the cold start error corrected simulation by ECHAM-1/LSG (*CORR*)

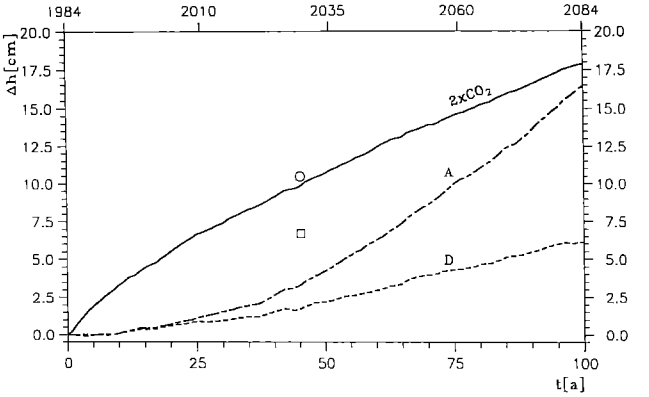

Fig. 11. Change of sea level height relative to the control simulation in the three ECHAM-1/LSG integrations (*lines*). "O" (best estimate) and "□" (low estimate) denote the IPCC scenario A estimates (thermal expansion only)

Table 3. Eigenvalue and amplitude of the response function for the temperature derived from the scenario A experiment, and the corresponding factor K_j

j	μ_j [a^{-1}]	α_j/μ_j [K]	K_j
1	1/36.8	2.246	0.243

(Fig. 10). The corrected curve approximates the best estimate of IPCC rather well. The remaining differences may be due to a genuine difference in the sensitivities of the ECHAM-1/LSG and the IPPC models, the internal variability of the coupled model or residual non-linear errors in the estimation of the response function (see Cubasch et al. 1992).

We applied also the new response function for an independent linear response calculation of the scenario D response (Fig. 9). Here the linear response model reproduces the initial warming during the first four decades reasonably well but fails, as before, to reproduce the ECHAM-1/LSG response for longer times. We suspect that this is again due to a non-linear positive feedback in the later stages of the scenario A simulation associated with the inhibition of heat transfer into the deep ocean as the climate is warmed. However, a more detailed analysis is needed to resolve this question. A good aggrement during the first 40 years nevertheless gives us some confidence that the cold start error inferred from the scenario A simulation (Fig. 7, dashed line) was computed correctly for this initial period in which the delay was most pronounced.

We also determined the impulse response function using as definition of the temperature change the instantaneous difference between the scenario A and the control simulations (definition 2 of Cubasch et al. 1992). The resulting parameters ($\alpha_1/\mu_1 = 2.60$ K, $\mu_1 = 1/36.3\, a^{-1}$) are very close to those used for our calculations (Table 3).

A shortcoming of our cold start error estimation is that the new response function is based on only a single scenario A simulation subject to natural initial climate variability. To confirm our result it is desirable to base the computation of the response function on a set of several scenario A experiments starting from different initial states.

In the case of the sea level rise the analysis was slightly modified as the internal variability appears to be more pronounced relative to the CO_2 induced increase. Thus, the change in the sea level was defined relative to the simultaneous sea level change in the control simulation (definition 2 of Cubasch et al. 1992) rather than relative to the sea level of the control simulation during the initial decade. Figure 11 shows the sea level rise due to thermal expansion of the ocean relative to the control simulation, for the three ECHAM-1/LSG simulations (Cubasch et al. 1992) and two IPCC estimates for scenario A (Houghton et al. 1990). The sea level signal is seen to be retarded even more strongly than the temperature response.

In contrast to the temperature, which is a signal from the uppermost ocean level, the sea level height represents an integral response of the entire ocean and for larger times is mostly determined by the warming of the deep ocean. In the "$2 \times CO_2$" experiment the deep ocean shows a more effective warming than in the scenario A simulation. This is due to the longer impact time of the sudden heat flux increase at time $t = t_b$ in the "$2 \times CO_2$" experiment compared with the slower increase of scenario A.

A good approximation of the simulated sea level response to a doubling of CO_2 (rms error 0.1 cm) can be obtained with two exponentials (Fig. 12),

$$R_h(t) = \sum_{j=1}^{2} \frac{h_j}{\nu_j}(1 - e^{-\nu_j t}) \tag{29}$$

with the parameters and partial factors listed in Table 4.

The resulting cold start error is plotted in Fig. 13. After 50 years the error is -3.7 cm (87% of the computed signal for scenario A) and -6.2 cm (31%) after 100 years. The cold start error explains about half of the delay of the ECHAM-1/LSG scenario A simulation relative to the IPCC estimate.

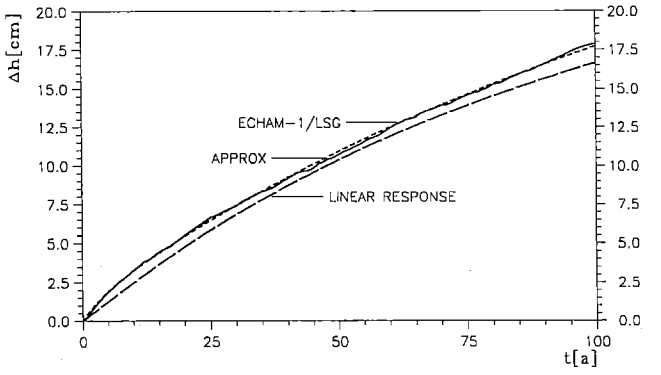

Fig. 12. Response the global height of sea level to an instantaneous CO_2 "doubling" ("$2 \times CO_2$" – "$1 \times CO_2$") for ECHAM-1/LSG (*full line*), and its approximation by a fit based on two exponentials (*APPROX, dotted line*) and by a linear response model based on scenario A (*LINEAR RESPONSE, dashed line*)

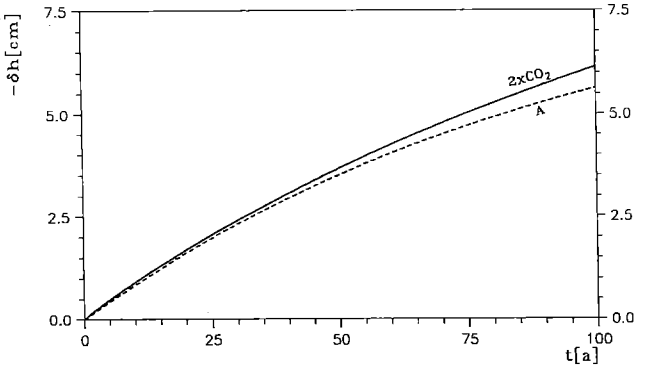

Fig. 13. Errors in sea level height due to the cold start for the model ECHAM-1/LSG based on the impulse response functions determined from the CO_2 "doubling" experiment (*solid line*) and from the scenario A simulation (*dashed line*)

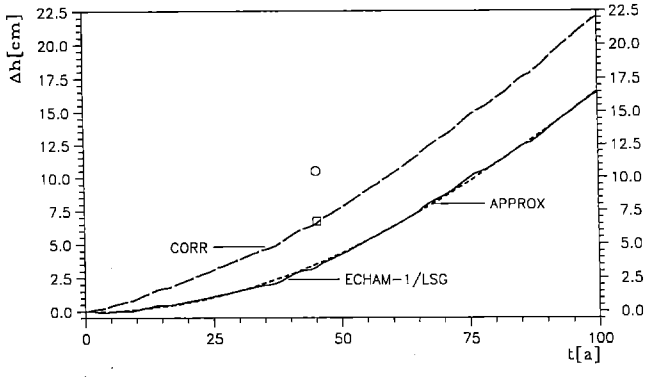

Fig. 14. Scenario A sea level rise relative to the control integration: simulation by ECHAM-1/LSG, approximation of the ECHAM-1/LSG curve by a fit (*APPROX*), and the cold start error corrected simulation by ECHAM-1/LSG (*CORR*). "O" (best estimate) and "□" (low estimate) denote the IPCC scenario A estimate (thermal expansion only)

Table 4. Eigenvalues and amplitudes of the response function for the sea level rise derived from the "$2 \times CO_2$" experiment, and the corresponding factors K_j

j	ν_j [a^{-1}]	h_j/ν_j [cm]	K_j
1	1/135.1	31.8	0.363
2	1/ 3.9	1.1	0.102

Table 5. Eigenvalue and amplitude of the response function for the sea level rise derived from the scenario A simulation, and the corresponding factor K_j

j	ν_j [a^{-1}]	h_j/ν_j [K]	K_j
1	1/99.0	26.2	0.339

The parameters and partial factor for the impulse response function for the sea level rise computed directly from the scenario A simulation are listed in Table 5. One exponential is sufficient to achieve an rms error of 0.1 cm (Fig. 14). The response function is very similar to the previous response function determined from the "$2 \times CO_2$" experiment (Fig. 12).

The resulting cold start error is plotted in Fig. 13. For a very long simulation time t the error approaches −8.9 cm. After correction for the cold start error, the ECHAM-1/LSG sea level response (Fig. 14) approaches the IPCC low estimate (square symbol in Fig. 14). Thus, most of the delay can be explained by the cold start error, but there remain also significant differences in the sea level rise due to thermal expansion computed using ECHAM-1/LSG, which includes the temperature and pressure dependence of the thermal expansion coefficient, and the box-diffusion-upwelling model (a more detailed discussion is given in Cubasch et al. 1992).

Application of the impulse response function determined from the scenario A simulation to compute the sea level rise for scenario D [in analogy with (28)] yields a rather good agreement with the simulation using the coupled ECHAM-1/LSG model (Fig. 15). Thus, in contrast to the temperature change, it appears that the sea level rise can be adequately described by a linear model which is valid for all CO_2 concentration scenarios.

5 Conclusions

We have applied a general linear response analysis to investigate the cold start problem inherent in all recent global warming simulations using coupled atmosphere-ocean models. The warming delay found by Cubasch et al. (1992) in their scenario simulations with the coupled model ECHAM-1/LSG can be attributed to a large part to the cold start error. It was found that the temperature response to a CO_2 doubling was too non-

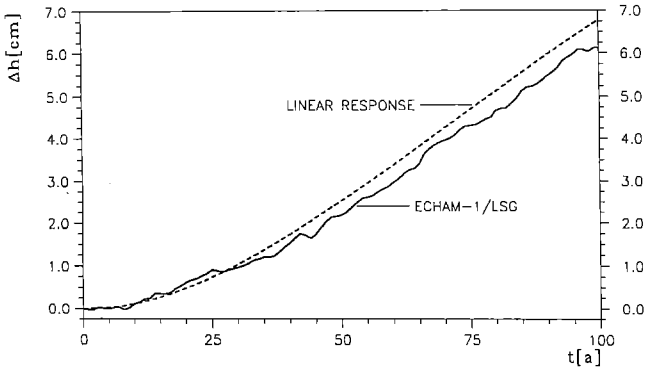

Fig. 15. Sea level response of ECHAM-1/LSG for scenario D (*solid line*), and its approximation by the linear response model (*dashed line*). The impulse response function is based on scenario A

linear to be used for determination of the impulse response function. This was therefore derived from the scenario A transient experiment. A comparison of the theoretical response for scenario D, computed using the new linear response function, with the coupled model response for scenario D suggests that even the response function inferred from the scenario A simulation may contain residual non-linearities for larger response times.

In the case of the sea level rise due to thermal expansion of the oceans, the cold start error explains approximately half of the reduction in the sea level rise of the coupled ECHAM-1/LSG model relative to the IPCC box-diffusion-upwelling model predictions for scenario A (best estimate). Both scenario A and the "$2 \times CO_2$" simulations yield very similar impulse response functions, so that the ECHAM-1/LSG model appears to behave more linearily with respect to the sea level rise than to temperature.

Acknowledgements. This work was sponsored by the Commission of the European Community, the Max-Planck-Gesellschaft, the Freie und Hansestadt Hamburg and the Deutsche Forschungsanstalt für Luft- und Raumfahrt. The authors would like to thank the staff of the Deutsches Klimarechenzentrum, the Meteorologisches Institut der Universität Hamburg and the Max-Planck-Institut für Meteorologie for their support. We also thank U. Cubasch and H. Höck for providing the temperature and sea level time series.

References

Cubasch U, Santer BD, Maier-Reimer E, Böttinger M (1990) Sensitivity of a global ocean atmosphere circulation model to a doubling of carbon dioxid. In: Pitcher EJ (ed) Science and engineering on supercomputers. Springer, Berlin Heidelberg Tokyo, pp 347–352

Cubasch U, Hasselmann K, Höck H, Maier-Reimer E, Mikolajewicz U, Santer BD, Sausen R (1992) Time-dependent greenhouse warming computations with a coupled ocean-atmosphere model. Clim Dyn 8:55–69

Houghton JT, Jenkins GJ, Ephraums JJ (1990) Climate change. The IPCC scientific assessment. Cambridge University Press, Cambridge, UK

Maier-Remier E, Hasselmann K (1987) Transport and storage of CO_2 in the ocean – an inorganic ocean-circulation carbon cycle model. Clim Dyn 2:63–90

Manabe S, Bryan K, Spelman MJ (1990) Transient response of a global ocean-atmosphere model to doubling of atmospheric carbon dioxide. J Phys Oceanogr 20:722–749

Stouffer RJ, Manabe S, Bryan K (1989) Interhemispheric asymmetry in climate response to a gradual increase of atmospheric CO_2. Nature 342:660–662

Washington WM, Meehl GA (1989) Climate sensitivity due to increased CO_2: experiments with a coupled atmosphere and ocean general circulation model. Clim Dyn 4:1–38

Wigley TMC (1991) A simple inverse carbon cycle model. Global Biogeochem Cycl 5:373–382